

IFUSP/P 704
B.L.F. - USP

UNIVERSIDADE DE SÃO PAULO

PUBLICAÇÕES

INSTITUTO DE FÍSICA
CAIXA POSTAL 20516
01498 - SÃO PAULO - SP
BRASIL

IFUSP/P-704

NUMERICAL INTEGRATION METHOD APPLIED TO THE
STUDY OF ATOMIC HYDROGEN IN α -Si:(H,O,N) AND
NATURAL BERYL DECAY KINETICS

26 MAI 1988



Wagner W. Furtado, Sadao Isotani, Rodolfo
Antonini, Ana Regina Blak and Walter Maigon
Pontuschka

Instituto de Física, Universidade de São Paulo

Março/1988

**NUMERICAL INTEGRATION METHOD APPLIED TO THE STUDY OF
ATOMIC HYDROGEN IN a-Si:(H,O,N) AND NATURAL BERYL
DECAY KINETICS**

ABSTRACT

A method of data processing was developed and applied to the study of decay kinetics of interstitial atomic hydrogen (H_1^0)¹ in X-irradiated a-Si:(H,O,N)² and natural beryl.

A system of differential kinetic equations was constructed considering multiple possible reactions. The solutions were evaluated by Runge-Kutta's method of numerical integration.

It was assumed that the H_1^0 was produced by radiolytic irradiation of R-H type molecules and trapped at interstitial sites of both materials. The heating releases the H^0 which quickly is either retrapped, recombined with R-radical left in the matrix or combined with other H^0 atoms forming H_2 molecules.

The parameters related to untrapping and recombination processes were found to obey Arrhenius law. On the other hand, the retrapping and H_2 -formation parameters were fit to a function proportional to $(T^{1/2} - T_0^{1/2})$, where at T_0 they vanish.

Wagner W. Furtado, Sadao Isotani, Rodolfo Antonini,
Ana Regina Blak and Walter Maigon Pontuschka

Instituto de Física, Universidade de São Paulo
C.P. 20516, 01498 São Paulo, SP, Brasil

PHYSICAL REVIEW B

PACS numbers:

76.30.Mi, 82.20.Pm, 82.20.-w, 02.60.+y, 76.30.-v,
61.80.-x, 61.80.Cb

ANA REGINA BLAK

Phone: 011-8155599 - Ramal 290 (BRASIL)

I. INTRODUCTION

Atomic hydrogen in natural crystals and amorphous materials has been studied by several authors [see references in 1]. Unfortunately, there are still very few systematic studies of the hydrogen centers isothermal kinetics. Recent studies in α -Si:(H,O,N)², natural beryl³, barium aluminoborate glasses⁴, and tourmaline⁵ report interesting results on atomic hydrogen thermal decay.

The H_1^0 observed in barium aluminoborate glasses⁴ is unstable at room temperature. The kinetics of this center was analysed in terms of the Levy's model⁶ yielding three first order processes, each one having a different activation energy. In contrast, the measured thermal decay of the H_1^0 in pink tourmaline⁵, stable at room temperature, follows a first order kinetics. A structural model was proposed to describe the trapping site of the atomic hydrogen in this crystal.

Pontuschka et al.² observed that the X-irradiated hydrogenated amorphous silicon containing oxygen and nitrogen impurities α -Si:(H,O,N) shows the characteristic H_1^0 doublet in the EPR spectrum. The absence of this center in X-irradiated nominally pure α -Si:H led to the conclusion that the presence of oxygen is needed to stabilize this center. A second order thermal decay kinetics was assumed in the analysis of the data yielding an activation energy of about 0.5 eV. Samples were

irradiated at room temperature till saturation. A series of EPR measurements was performed to study the isothermal decay of the atomic hydrogen centers. The measurements were carried out at 310, 319, 323, 332 and 343K, respectively.

Atomic hydrogen, stable at room temperature, was observed in X-irradiated beryl by Koryagin and Grechushnikov⁷ in 1966 and by Bershov⁸ in 1970. When beryl was completely dehydrated, H_1^0 was not detected, leading to the conclusion that it is originated from the H_2O radiolysis⁷. Blak et al.⁹ also observed EPR of H_1^0 centers in beryl, UV-irradiated at room temperature, in 1982. Isothermal decay measurements at 353, 373, 393, 413, 433 and 453K could not be described in terms of first or second order kinetics¹³. This suggests the need of considering the superposition of several kinetic processes occurring together. It is not difficult to write down the differential equation for each possible reaction.

However, exact solutions of systems of chemical kinetics differential equations can easily become laborious or even prohibitive in most cases. For this reason one resorts to numerical integration which, with the present day easy access to personal computers, is quite manageable.

II. THE KINETIC EQUATIONS

We assume that atomic hydrogen is produced during UV and X-irradiation of beryl and α -Si:(H,O,N) samples by photo-dissociation of R-H type molecules leaving H^0 and R radicals. In beryl, R is assumed to be OH^- , from dissociation of H_2O and in α -Si:(H,O,N), R is part of the disordered chain of its amorphous structure during irradiation. The H^0 diffuses throughout the interstices of the network before being recombined or trapped in stabilizing sites. After sufficient time of irradiation, all the available traps are filled and the growth of interstitial atomic hydrogen $[H_i^0]$ (the brackets are referred to as concentration) reaches saturation. In the following, the subsequent notation will be adopted:

R : recombination center;

H : trapping site;

H_t : trapped H_i^0 ;

H_f : free H_i^0 diffusing throughout the sample;

RH : molecules;

S : empty traps.

On heating, the H_t overcomes the energy barrier and moves throughout the lattice interstices prior to the reactions of retrapping, recombination, or combination of two H_f forming H_2 molecule.

The change rates of $[H_t]$, $[H_f]$, $[S]$, $[R]$, $[RH]$ and $[H_2]$ are described by the following differential equations:

$$\frac{d}{dt} [H_t] = -\alpha[H_t] + \gamma[H_f][S] \quad (1a)$$

$$\frac{d}{dt} [H_f] = \alpha[H_t] - \gamma[H_f][S] - \beta[H_f][R] - \delta[H_f]^2 \quad (1b)$$

$$\frac{d}{dt} [S] = \alpha[H_t] - \gamma[H_f][S] \quad (1c)$$

$$\frac{d}{dt} [R] = -\beta[H_f][R] \quad (1d)$$

$$\frac{d}{dt} [RH] = \beta[H_f][R] \quad (1e)$$

$$\frac{d}{dt} [H_2] = \delta[H_f]^2 \quad (1f)$$

where α , β , γ and δ are adjustable parameters.

The number of H_i trapping sites is assumed to be constant

$$[H_t] + [S] = [N] \quad (2)$$

where $[N]$ is the concentration of trapping sites.

From the equations (1d) and (1e) we observe that the sum of $[R]$ and $[RH]$ is constant. The equations (1e) and (1f) are independent of the others and may therefore be solved separately.

The system is then reduced to the following coupled kinetics equations:

$$\frac{d}{dt} [H_t] = -\alpha[H_t] + \gamma[H_f] \{N - [H_t]\} \quad (2a)$$

$$\frac{d}{dt} [H_f] = \alpha[H_t] - \gamma[H_f] \{N - [H_f]\} - \beta[H_f][R] - \delta[H_f]^2 \quad (2b)$$

$$\frac{d}{dt} [R] = -\beta[H_f][R] \quad (2c)$$

The above equations were normalized assuming that all sites are filled. The initial conditions are given by: $N=1$, $[H_t](0)=1$, $[H_f](0)=0$ and $[R](0)=1$. The coupled differential equations (2) were solved using the numerical method of Runge-Kutta¹⁰⁻¹².

The Runge-Kutta's method is especially suited to solve numerically a system of first order differential equations. Among the advantages of this method it is important to see that it is not necessary to calculate derivatives as in Taylor series, since the calculation of (n+1)th functional value y_{n+1} depends only on the value of the nth function y_n .

The error in this method can be evaluated as the sum over all step errors assuming all of them being equal for each iteration. For n points iteration, the error in the nth point is $\epsilon_n = \sum_{i=1}^n \epsilon_i = n\epsilon_1$.

III. RESULTS

The experimental values used in this work are the same published by Pontuschka¹² and Blak¹³. The coupled differential equations (2) were numerically solved with parameters fitted by trial and error method, after a few iterations. Once the motion of the H_f is such that the mean time between collisions is too short to enable the H_f be detected by EPR, the EPR signal intensity was attributed only to the H_t .

We start studying the curve dependence for small variations in each of the previously adjusted parameters α , β , γ , and δ , the others remaining constant at a given temperature. In Figure 1, the solid line corresponds to the best fit obtained for $\alpha=24.0$, $\beta=1.0$, $\gamma=41.0$ and $\delta=15.5$ in beryl at 413K. The dotted and dashed lines represent the effect of the parameter change on the calculated thermal decay, respectively, for α (Figure 1a), β (Figure 1b), γ (Figure 1c) and δ (Figure 1d).

INSERT FIGURE 1

The numerical integration results (solid lines) adjusted to the experimental points for the isothermal decay of atomic hydrogen for X-irradiated a-Si:(H,O,N) is shown in Figure 2 where β was assumed to be zero. The best

 INSERT FIGURE 2

fit parameters are shown in Table I. The results of our calculations

 INSERT TABLE I

are in good agreement with the assumption proposed by Pontuschka et al.² ascribing the principal process involved in the removal of hydrogen from a-Si:H as the formation of H₂. Figure 3 shows the Arrhenius law applied to α parameter. The activation

 INSERT FIGURE 3

energy is $E_{\alpha} = 0.56$ eV and the pre-exponential frequency factor $\alpha_0 = 1.5 \times 10^9$ s⁻¹.

The best fit (solid lines) for the [H_t] decay of UV-irradiated beryl is shown in Figure 4. The β -value was no

 INSERT FIGURE 4

longer negligible as occurred for a-Si:(H,O,N). The calculated parameters are listed in Table II. In Figure 3 it is clear that

 INSERT TABLE II

both parameters α and β obey Arrhenius law with activation

energies respectively equal to $E_{\alpha} = 0.42$ eV and $E_{\beta} = 1.51$ eV and pre-exponential frequency factors $\alpha_0 = 3.33 \times 10^6$ s⁻¹ and $\beta_0 = 3.48 \times 10^{18}$ s⁻¹.

IV. DISCUSSION

Concerning the changes in the isothermal decay curve, caused by variations in the parameters α , β , γ , and δ , our calculations led to the following observations:

a) An increase in the untrapping parameter α produces a faster isothermal decay. As the behavior of this parameter is expected to obey Arrhenius law, $\alpha = \alpha_0 \exp(-E_{\alpha}/kT)$, where E_{α} is the activation energy, it is clear that the shallower the trap, the faster the decay (Figure 1a).

b) In the case of the recombination parameter β , it is also observed that an increase in this parameter induces a faster isothermal decay, associated with an increased recombination probability (Figure 1b).

c) The retrapping parameter γ produces a trend opposite to the isothermal decay. The increased value of γ decreases the thermal decay rate, since it contributes to restore the trapped hydrogen population (Figure 1c).

d) The H_2 -formation parameter δ , when increased, accelerates the isothermal decay as expected from an increased rate of H_2 production (Figure 1d).

When H_t is released from its trap, transforming in H_f , it behaves like a free atom, forming a gas-like system and in this case we can apply the concepts of the elementary theory of gas kinetics. As the parameters γ and δ are products of collision cross-sections \times velocities of moving particles, their value increases with temperature as expected. The speed distribution for the diffusion of H_f throughout the material network is temperature dependent. Thus, analysing the speed distribution, allows us to sketch a temperature dependence for these parameters.

Let us assume again that H_f behaves like a free atom, forming a gas-like system of H_f^0 atoms with effective mass m_H . The density of atoms varies accordingly the Maxwell speed distribution

$$dN = \frac{4N}{\sqrt{\pi}} \left(\frac{m_H}{2kT} \right)^{3/2} v^2 \exp \left(-\frac{m_H v^2}{2kT} \right) dv \quad (3)$$

where N is the concentration of H_f atoms, v the speed and T the absolute temperature. Consider N_v atoms per unit volume travelling in the network with speed between v and $v+dv$. By assuming that each collision with atoms N' removes one H_f

atom, we may evaluate the rate of decreasing of N_v between t and $t+dt$ according to:

$$dN_v = -PN_v dx \quad (4)$$

where $P = \sigma N'$, σ = cross section and $dx = vdt$. The rate of change of concentration for all speeds is then given by the sum over all dN_v , giving:

$$\frac{dN}{dt} = -\sigma N' \int_{\text{all}} v dN \quad (5)$$

Using the equation (3), we obtain the rate equation:

$$\frac{dN}{dt} = -\sigma \bar{v} N N' \quad (6)$$

where $\bar{v} = (8kT/\pi m_H)^{1/2}$. This result yields $T^{1/2}$ behavior for the parameters γ and δ .

Figure 5 shows the correlation of γ and δ for $[H_t]$ in a-Si:(H,O,N) with $T^{1/2}$. The observed correlation is

INSERT FIGURE 5

linear, with a common cutoff temperature $T_0 = 269K$ for all the parameters. Thus, γ and δ are linear functions of $(T^{1/2} - T_0^{1/2})$.

The dependence of γ and δ for $[H_t]$ in beryl on $T^{1/2}$ is shown in Figure 6. The behavior is again linear, with

 INSERT FIGURE 6

cutoff temperature $T_0 = 266\text{K}$ and here again γ and δ are linear functions of $(T^{1/2} - T_0^{1/2})$.

In Figure 3 it is shown that the parameter β , adjusted to the kinetics of $[H_t]$ in beryl, obeys Arrhenius law. The parameter β is related to the recombination process of R and H_f . The high activation energy suggests that the irradiation produced an R radical from the radiolysis of H_2O , namely OH^- . Therefore, the activation energy is probably equal to the energy necessary for the ionization of OH^- into $OH + e^-$ before the reaction $OH + H_f \rightarrow H_2O$ took place. An alternative possible reaction is $OH^- + H_f \rightarrow H_2O^-$
 $H_2O^- \rightarrow H_2O + e^-$.

IV. SUMMARY

Numerical Runge-Kutta's method, applied to a system of differential equations describing the isothermal decay kinetics of $[H_t]$ in X-irradiated a-Si:(H,O,N) and UV-irradiated natural beryl, led to conclusions which can be summarised as below.

a) The hydrogen removal mechanism which occurs on heating a-Si:H is processed through the irreversible formation of molecular H_2 , in good agreement with the assumption proposed by Pontuschka et al.². In this work it is assumed that the

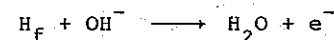
reaction $H_f + H_f \rightarrow H_2$ has zero activation energy (absence of potential barrier).

b) The untrapping of H_t in a-Si:(H,O,N) obeys Arrhenius law with activation energy $E_\alpha = 0.56\text{ eV}$ and pre-exponential factor $\alpha_0 = 1.5 \times 10^9\text{ s}^{-1}$.

c) The recombination parameter β is negligible for H_f in a-Si:(H,O,N) (it is unlikely that the radiolytic H_f be recovered in the original structure).

d) The recombination parameter β is not negligible for H_f in beryl, a fact which minimizes the loss of hydrogen by the sample.

e) Both α (untrapping) and β (recombination) parameters obey Arrhenius law for beryl with activation energies respectively equal to $E_\alpha = 0.42\text{ eV}$ and $E_\beta = 1.51\text{ eV}$ and pre-exponential factors respectively equals to $\alpha_0 = 3.33 \times 10^6\text{ s}^{-1}$ and $\beta_0 = 3.48 \times 10^{18}\text{ s}^{-1}$. The recombination of H_f in beryl, processed through the reaction



justifies the high E_β activation energy ($E_\beta = 1.51\text{ eV}$).

f) The parameters γ (retrapping) and δ (H_2 formation) were found to fit a function proportional to $(T^{1/2} - T_0^{1/2})$ with cutoff energy $T_0 = 269\text{K}$ for H_f in a-Si:(H,O,N) and $T_0 = 266\text{K}$ in beryl.

ACKNOWLEDGMENTS:

We wish to thank Dr. E.F. Pessoa for many useful discussions. This work was partly supported by grants from the Conselho Nacional de Desenvolvimento Científico (CNPq) and from the Financiadora de Estudos e Projetos (FINEP).

REFERENCES

1. R. Livingstone, H. Zeldes, and E.H. Taylor, *Disc. Faraday Soc.*, 19, 166 (1955); B. Smaller, M.S. Matheson, and E.L. Yasaitis, *Phys. Rev.*, 94, 202 (1954); C.J. Delbecq, B. Smaller, and P.H. Yuster, *Phys. Rev.*, 104, 599 (1956); E.L. Cochran, V.A. Bowers, S.N. Foner, and C.K. Jen; *Phys. Rev. Lett.*, 2, 43 (1959); J.L. Hall and R.T. Schumacher, *Phys. Rev.*, 127, 1982 (1962); B. Welber, *Phys. Rev.*, 136A, 1408 (1964); R.G. Bessent, W. Hayes, and J.W. Hodby, *Phys. Lett.*, 15, 115 (1965); R.B. Bessent, W. Hayes, and J.W. Hodby, *Proc. Roy. Soc.*, A297, 376 (1967); C.K. Jen, S.N. Foner, E.L. Cochran, and V.A. Bowers, *Phys. Rev.*, 104, 846 (1956); C.K. Jen, S.N. Foner, E.L. Cochran, and V.A. Bowers, *Phys. Rev.*, 112, 1169 (1958); F.J. Adrian, *J. Chem. Phys.*, 32, 972 (1960); S.N. Foner, E.L. Cochran, V.A. Bowers, and C.K. Jen, *J. Chem. Phys.*, 32, 963 (1960); D.Y. Smith, *Phys. Rev.*, 131, 2056 (1963); D.Y. Smith, *Phys. Rev.*, 133A, 1087 (1964); R.A. Weeks and M. Abraham, *J. Chem. Phys.*, 42, 68 (1965); B. Welber, *J. Chem. Phys.*, 43, 3015 (1965); S. A. Marshall, and J.R. Gabriel, *J. Chem. Phys.*, 45, 192 (1966); R.G. Bessent, W. Hayes, J.W. Hodby, and P.H.S. Smith, *Proc. Roy. Soc.*, A309, 66 (1969); J. Helbert and L. Kevan, *J. Chem. Phys.*, 58, 1205 (1973); B.D. Perlson and J.A. Weil, *J. Mag. Res.*, 15, 594 (1974); M. Bowman, L. Kevan, and R.N. Schwartz, *Chem. Phys. Lett.*, 30, 208 (1975); N. Papp and K.P. Lee, *J.*

- Mag. Res., 12, 245 (1975); A. Edgar and E.R. Vance, Phys. Chem. Minerals, 1, 165 (1977).
2. W.M. Pontuschka, W.W. Carlos, P.C. Taylor, and R.W. Griffith, Phys. Rev. B25, 4362 (1982).
 3. A.R. Blak, W.M. Pontuschka, and S. Isotani, "International Conference on Defects in Insulating Crystals", Univ. Utah, Salt Lake City, 43 (1984).
 4. W.M. Pontuschka, S. Isotani, and A. Piccini, J. Am. Cer. Soc., 65, 519 (1982).
 5. M.B. Camargo, Ph.D. Thesis, Institute of Physics, University of São Paulo (1985).
 6. P.W. Levy, P.L. Mattern, K. Lengweiler, and A.M. Bishay, J. Am. Ceram. Soc., 57, 176 (1974).
 7. V.F. Koryagin and B.N. Grechushnikov, Sov. Phys. Sol. Stat., 7, 2010 (1966).
 8. L.V. Bershov, Geochemistry, 7, 853 (1970).
 9. A.R. Blak, S. Isotani, and S. Watanabe, Rev. Bras. Fís., 12, 285 (1982).
 10. W.E. Milne, in "Numerical Solution of Differential Equations", edited by Dover Publications, Inc., New York (1970).
 11. L. Brand, in "Differential and Difference Equations", edited by John Wiley & Sons, Inc., New York, London, Sydney (1966).
 12. W.E. Boyce and R.C. Di Prima, in "Elementary Differential Equations and Boundary Value Problems", edited by John Wiley & Sons, Inc., New York, London, Sydney (1977).

13. A.R. Blak, W.M. Pontuschka, and S. Isotani, An. Acad. Brasil. Ci., 60(1) (1988). In print.

FIGURE CAPTIONS

FIGURE 1 - Isothermal $[H_t]$ decay curve dependence for small variations in the adjusted parameters α (FIG. 1A), β (FIG. 1B), γ (FIG. 1C), and δ (FIG. 1D), in beryl at 413 K¹³.

FIGURE 2 - Numerical integration results (solid lines) adjusted to the experimental points of the isothermal $[H_t]$ decay in a-Si:(H,O,N)¹².

FIGURE 3 - Arrhenius law applied to the parameters α and β for beryl and α for a-Si:(H,O,N).

FIGURE 4 - Numerical integration results (solid lines) adjusted to the experimental points of the isothermal $[H_t]$ decay in beryl¹³.

FIGURE 5 - The $T^{1/2}$ behavior observed for the γ and δ parameters of $[H_t]$ in a-Si:(H,O,N). The common cutoff temperature is $T_0 = 269K$.

FIGURE 6 - The $T^{1/2}$ behavior observed for the γ and δ parameters of $[H_t]$ in beryl. The common cutoff temperature is $T_0 = 266K$.

TABLE I - Parameters α , γ and δ for a-Si:(H,O,N).

T(K)	α	γ	δ
310	1.25 $\begin{smallmatrix} +0.03 \\ -0.05 \end{smallmatrix}$	28.5 $\begin{smallmatrix} +3.5 \\ -1.5 \end{smallmatrix}$	165 $\begin{smallmatrix} +5 \\ -25 \end{smallmatrix}$
323	2.9 $\begin{smallmatrix} +0.2 \\ -0.2 \end{smallmatrix}$	37.5 $\begin{smallmatrix} +1.5 \\ -2.5 \end{smallmatrix}$	215 $\begin{smallmatrix} +15 \\ -10 \end{smallmatrix}$
332	5.1 $\begin{smallmatrix} +0.4 \\ -0.3 \end{smallmatrix}$	43.5 $\begin{smallmatrix} +2.5 \\ -4.5 \end{smallmatrix}$	250 $\begin{smallmatrix} +20 \\ -20 \end{smallmatrix}$
343	7.0 $\begin{smallmatrix} +0.5 \\ -1.0 \end{smallmatrix}$	51 $\begin{smallmatrix} +9 \\ -11 \end{smallmatrix}$	295 $\begin{smallmatrix} +35 \\ -65 \end{smallmatrix}$

TABLE II - Parameters α , β , γ and δ for beryl.

	α	β	γ	δ
353	3.45 $\begin{smallmatrix} +0.15 \\ -0.15 \end{smallmatrix}$	-	24.5 $\begin{smallmatrix} +1.0 \\ -1.0 \end{smallmatrix}$	9.8 $\begin{smallmatrix} +0.8 \\ -0.8 \end{smallmatrix}$
373	6.7 $\begin{smallmatrix} +0.2 \\ -0.2 \end{smallmatrix}$	-	30.0 $\begin{smallmatrix} +1.0 \\ -1.0 \end{smallmatrix}$	11.5 $\begin{smallmatrix} +1.0 \\ -0.7 \end{smallmatrix}$
393	13.8 $\begin{smallmatrix} +0.6 \\ -0.4 \end{smallmatrix}$	0.14 $\begin{smallmatrix} +0.05 \\ -0.03 \end{smallmatrix}$	35.0 $\begin{smallmatrix} +1.5 \\ -0.5 \end{smallmatrix}$	13.5 $\begin{smallmatrix} +0.5 \\ -1.0 \end{smallmatrix}$
413	24.0 $\begin{smallmatrix} +0.5 \\ -0.5 \end{smallmatrix}$	1.0 $\begin{smallmatrix} +0.2 \\ -0.1 \end{smallmatrix}$	41.0 $\begin{smallmatrix} +1.0 \\ -1.0 \end{smallmatrix}$	15.5 $\begin{smallmatrix} +0.5 \\ -0.9 \end{smallmatrix}$
433	44 $\begin{smallmatrix} +2 \\ -1 \end{smallmatrix}$	6 $\begin{smallmatrix} +1 \\ -1 \end{smallmatrix}$	46.0 $\begin{smallmatrix} +0.5 \\ -1.0 \end{smallmatrix}$	17.0 $\begin{smallmatrix} +0.5 \\ -0.5 \end{smallmatrix}$
453	72 $\begin{smallmatrix} +2 \\ -6 \end{smallmatrix}$	20 $\begin{smallmatrix} +1 \\ -2 \end{smallmatrix}$	50.0 $\begin{smallmatrix} +0.8 \\ -0.8 \end{smallmatrix}$	19.0 $\begin{smallmatrix} +0.8 \\ -0.6 \end{smallmatrix}$

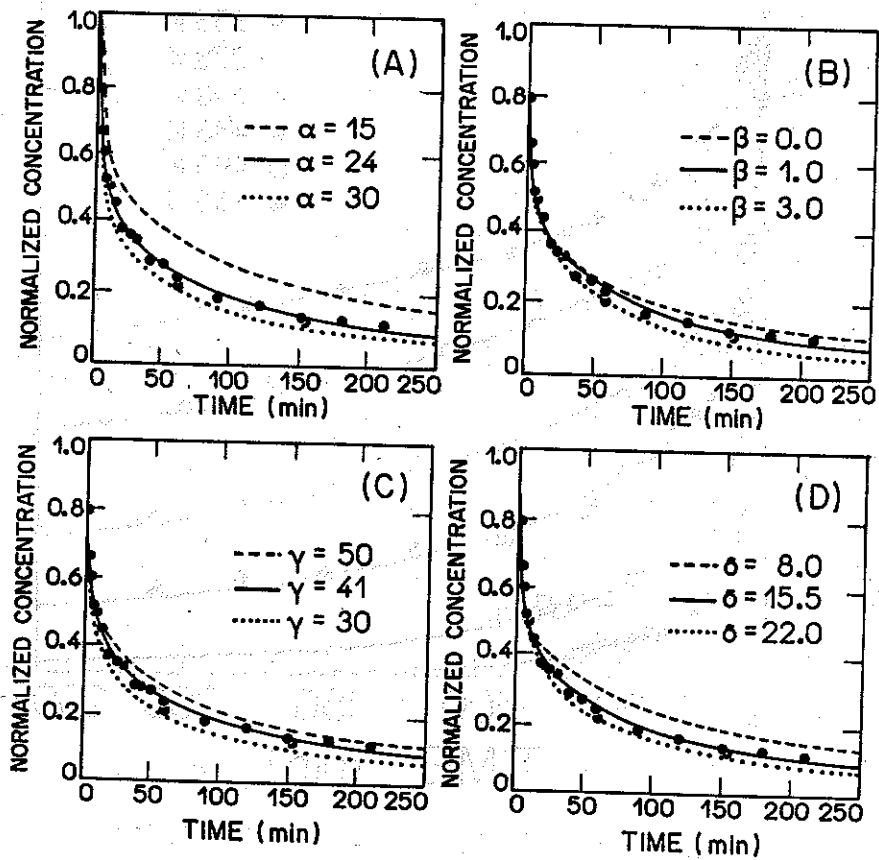


Figure 1

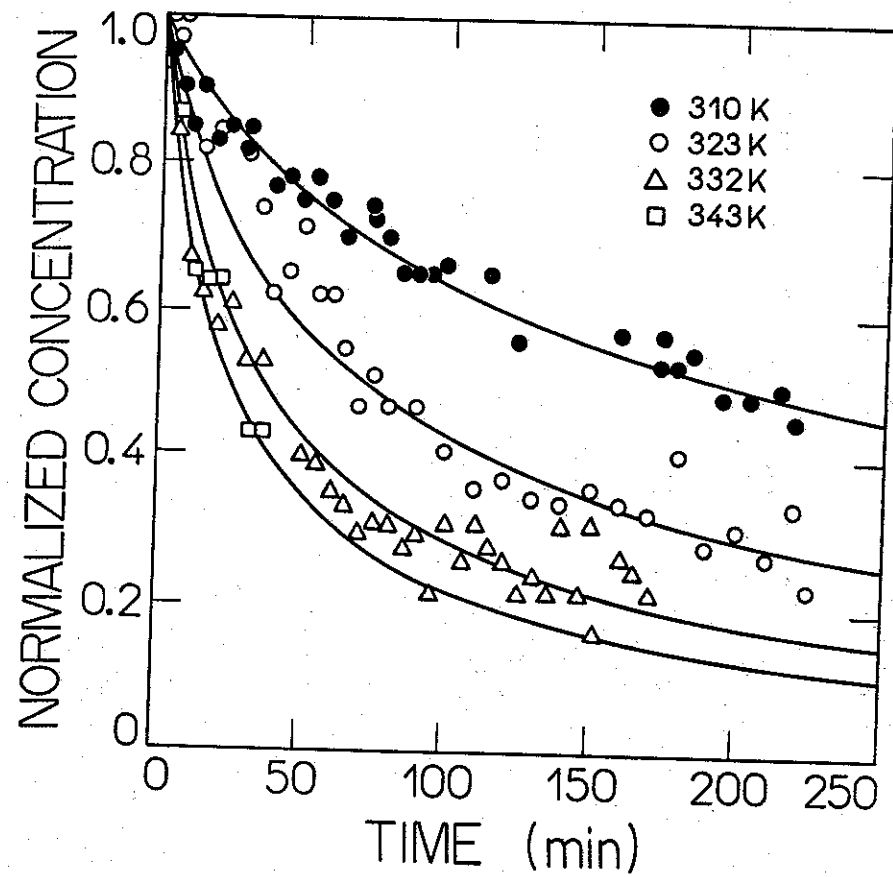


Figure 2

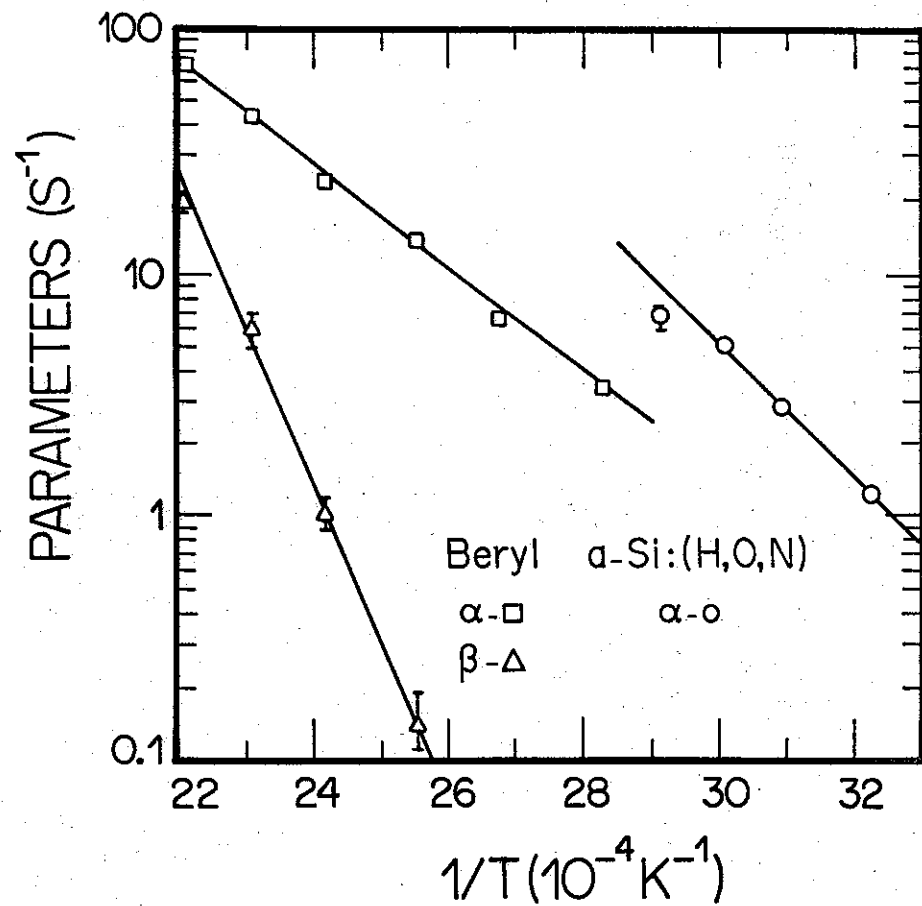


Figure 3

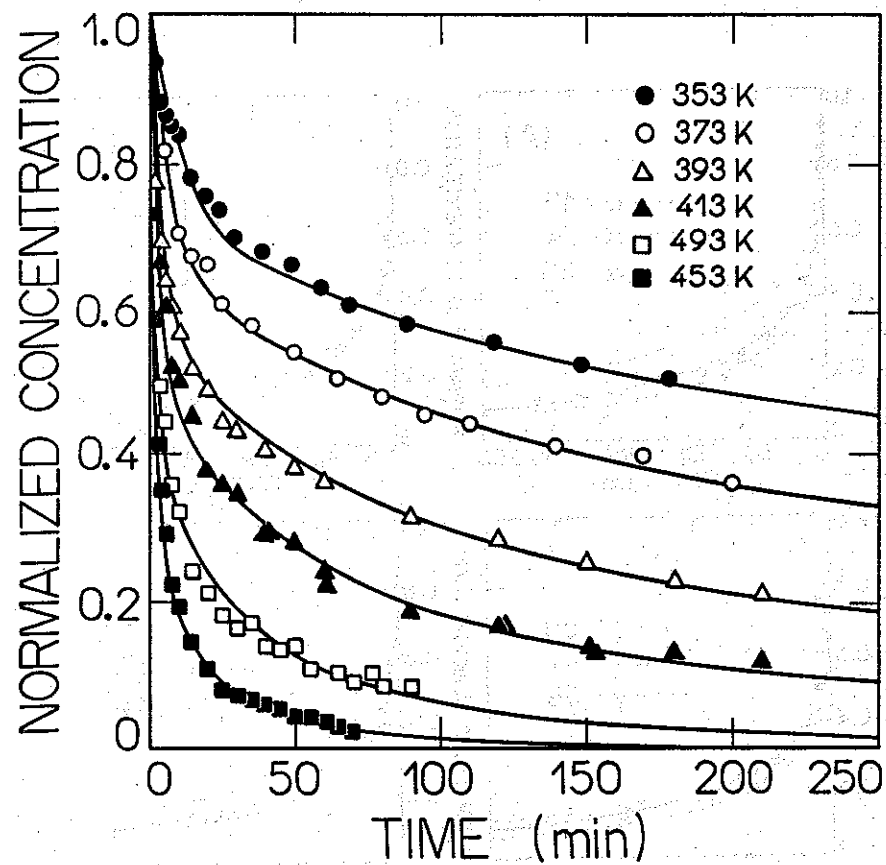


Figure 4

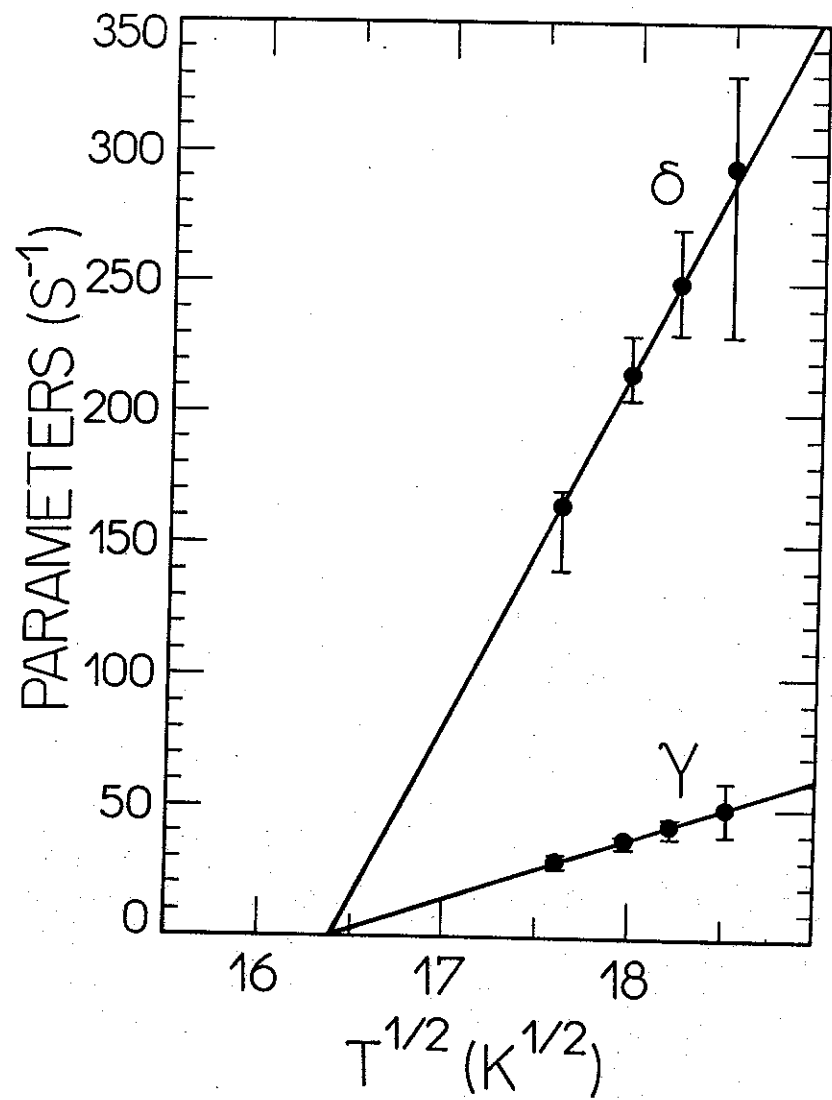


Figure 5

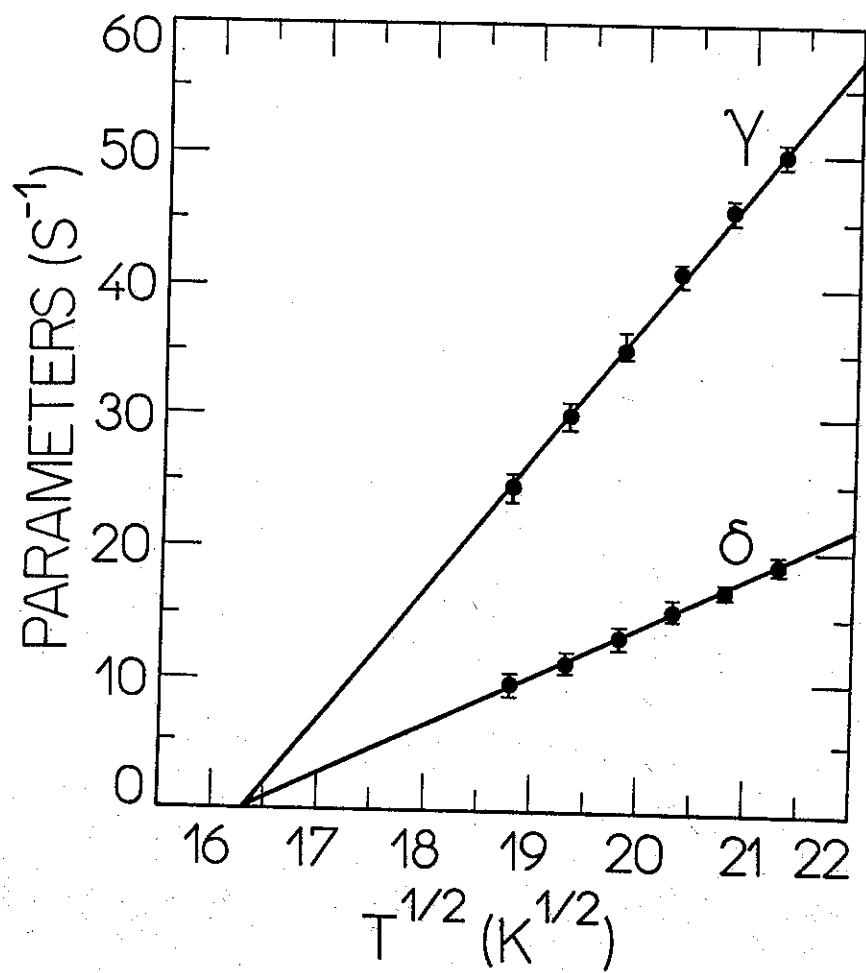


Figure 6